The development and application of synthetic affinity ligands for the purification of ferritin-based influenza antigens

Shaleem I. Jacob[*,†]

Basmah Khogeer[†]

Nick Bampos[‡]

Tom Sheppard[Ψ]

Richard Schwartz[§]

Christopher R. Lowe[†]

[†] Department of Chemical Engineering and Biotechnology, University of Cambridge, Cambridge, UK

[‡] Department of Chemistry, University of Cambridge, Cambridge, UK

[Ψ] Department of Chemistry, University College London, London, UK

[§] Vaccine Production Program Laboratory, National Institute of Health, Gaithersburg, USA

*Corresponding author at: Department of Biochemical Engineering, University College London, Bernard Katz Building, Gower Street, London, WC1E 6BT

Email address: shaleem.jacob@gmail.com

Mobile: +447595751656

Abstract

A recently developed novel recombinant influenza antigen vaccine has shown great success in pre-clinical studies in ferrets and mice. It provides broader protection, and is efficient to manufacture compared to the conventional trivalent influenza vaccines (TIV). Each strain of the recombinant antigen has a constant self-assembled bacterial ferritin core which, if used as a target for affinity chromatography, could lead to a universal purification method. Ferritin *in silico* models were used to explore potential target binding sites against ligands synthesised by the four-component Ugi reaction. Two ligands, SJ047 and SJ055, were synthesised in solution, characterised by ^{1}H-, ^{13}C- and 2D-NMR spectroscopy, and subsequently immobilised on the PEG-functionalised beads. Ligands SJ047 and SJ055 displayed apparent K_d values of 2.04×10^{-7} M and 1.91×10^{-8} M, respectively, against the ferritin. SJ047 and SJ055-functionalised resins were able to purify haemagglutinin (New Caledonia)-ferritin expressed in a crude Human Embryonic Kidney (HEK) cell supernatant in a single step to a purity of 85±0.5% (97±1% yield) and 87.5±0.5% (95.5±1.5% yield), respectively. Additionally, SJ047 and SJ055-functionalised resins purified the recombinant antigens when spiked at known concentrations into HEK supernatants. All three strains, haemagglutinin (New Caledonia)-ferritin, haemagglutinin (California)-ferritin and haemagglutinin (Singapore)-ferritin were purified, thereby offering an ideal alternate platform for affinity chromatography. Following elution from the affinity adsorbents, absorbance at 350 nm showed that there was no aggregation of the recombinant antigens and dynamic light scattering studies further confirmed the structural integrity of the recombinant antigen. The use of Ugi ligands coupled to a PEG-spacer arm to target the ferritin core of the strain is entirely novel and provides an efficient purification of these recombinant antigens. This approach represents a potentially universal method to purify any ferritin-based vaccine.

Introduction

The influenza A virus has claimed the lives of more than 50 million people in the past 100 years.[1] Annually, almost 250 million doses of influenza vaccine are brought to market in more than 100 countries.[2] The manufacturer CSL estimated the market for influenza vaccines at US$4 billion.[3] The genetic capability of the influenza virus to mutate annually increases pressure on manufacturers to produce and stockpile influenza vaccines.

Recently, several seasonal viral vaccines have moved away from an egg-based process and have adopted a recombinant approach. The main reason for this change is to prevent vaccine production issues attached with embryonated eggs (i.e. shortage of egg supply in the event of any avian disease outbreak) and the suitability for patients with egg allergies.[4] These advantages of recombinant antigen vaccines led Kanekiyo and co-workers to develop a mammalian cell culture based recombinant antigen vaccine.[5] The manufacturing process takes approximately 7 weeks.[6]

Furthermore, downstream processing of biological products accounts for over 50-80% of the total production costs,[7] and thus alternative efficient purification methods can be used to reduce manufacturing costs significantly. Affinity chromatography binds the target protein reversibly but with high specificity. This means that high purity can be achieved in one step compared to the same purity being achieved in a purification chain. Synthetic affinity ligands are ideally suited to the purification of high value biopharmaceutical proteins since they are inexpensive, chemically defined, exhibit increased stability, display reuse potential, are non-toxic, contain no fissile bonds, and are highly selective and resistant to degradation.[8]

The two most widely used isocyanide-based multicomponent reactions are the Passerini three-component reaction to produce α-acyloxy carboxamides and the Ugi four-component reaction, which yields α-acylamino carboxamides.[9] Ugi multi-component reactions (MCR) mimic

dipeptide scaffolds and therefore they can make good synthetic affinity ligands for purifying proteins.[10] Synthetic ligands using a combinatorial approach have been successfully used in affinity chromatography at a small scale for a wide variety of biomolecules including immunoglobulins,[10] glycoproteins,[11] recombinant human erythropoietin,[12] recombinant insulin precursor MI3 and human recombinant factor VIIa.

The present research aims to purify three different strains of the HA-ferritin antigen (Figure 1). The constant domain ferritin will be targeted by the multicomponent Ugi affinity ligand. However, as ferritin is the core of the protein, the interaction between the ligand coupled Sepharose™ and ferritin represents a steric challenge. Therefore, a long spacer arm was coupled to the resin to enable better accessibility to the ferritin. Polyethene glycol diglycidyl ether (PEG-DE) of approximately 120Å[13] was conjugated to the support in order to improve the efficiency of binding with the ferritin residues for a platform affinity purification of different HA strains (Figure 1).

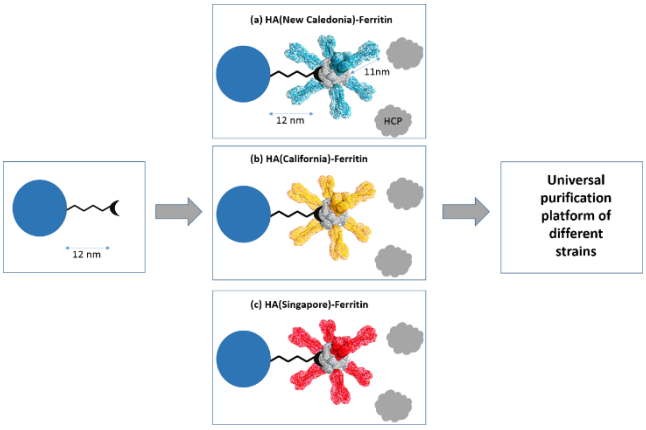

Figure 1. Affinity purification of three different HA-ferritin strains. (a) Sepharose conjugated to Ugi functionalised PEG-DE (120Å) targeting the ferritin core to purify HA (New Caledonia)-Ferritin from the human embryonic kidney (HEK) cell supernatant containing host cell protein (HCP) impurities. The ligand has the same ferritin target site, therefore, it can purify (b) HA (California)-ferritin and (c) HA (Singapore) from the HEK cell supernatant.

Results and discussion

Rational Approach to Ugi-ligand design. Rational design is effective when the structure and mechanism of the protein are well known and documented.[14] The HA-ferritin was generated by fusing the ectodomain of HA to *Helicobacter pylori* ferritin with a Ser-Gly-Gly linker (Figure 1).[5] Haemagglutinin (HA) is a well-studied antigenic glycoprotein with at least 18 subtypes. However, due to the differences in structure of the various subtypes of HA, ligand generation was based on complementarity with the constant ferritin domain of the HA-ferritin vaccine. Therefore, the crystallographic structure of *Helicobacter pylori* ferritin was obtained from the protein database (PDB code: 3EGM); this enabled the study of the interactions between the ferritin exposed residues and the ligand to be modelled *in silico*. Ferritin is composed of 24 subunits to form a naturally assembled cage architecture (Figure 2a).[15] Both individual ferritin subunits and multiple assembled subunits were modelled to provide an insight into the three-dimensional space of individual subunits, the accessibility of potential hydrophobic binding pockets and their complementarity to the proposed synthetic ligands (Figure 2).

First, hydrophobic binding pockets on one ferritin subunit were analysed (Figure 2b), and the ligand was docked into the most accessible pocket. CLC drug discovery workbench modelled six hydrophobic binding pockets of different sizes on the ferritin subunit. The least accessible hydrophobic binding pockets of volumes 41.98Å^3, 29.18Å^3 and 26.11 Å^3 were closest to the NH_2-terminus because the trimeric HA was fused to the ferritin at aspartic acid (Asp^5). Thus, the ligand interaction with these three pockets was considered unlikely due to the steric demands of the HA. In addition, the other two hydrophobic pockets of volumes 20.48Å^3 and 84.48Å^3 were positioned away from the ferritin surface and located near the ferritin core; hence, there was a very low possibility of ligand interaction in this area. The most accessible hydrophobic binding pocket was the one furthest away from the NH_2-terminus and the

protruding HA spikes. This pocket had a size of 30.72Å^3 and was located near the loop region on the surface of the ferritin subunit. We recognise, however, that there is potential for the ligands to bind to the other binding pockets, and this could have either a beneficial or detrimental impact on the purification. The chance of capture is higher due to the avidity effects caused my multiple binding interactions due to the increased binding sites.[16] This effect can increase the potential binding onto the column; however, the elution of the recombinant antigen may prove difficult.

Nevertheless, ferritin was modelled (Figure 2c) to observe the putative binding regions of the oligomeric structure using CLC drug discovery. The charged residues on the surface were also analysed (Figure 2d), thereby evaluating the accessibility of the target hydrophobic region for the synthesised ligands. The target binding regions were displayed on the surface and ligand SJ047 was docked in this region (Figure 2d and Figure 3).

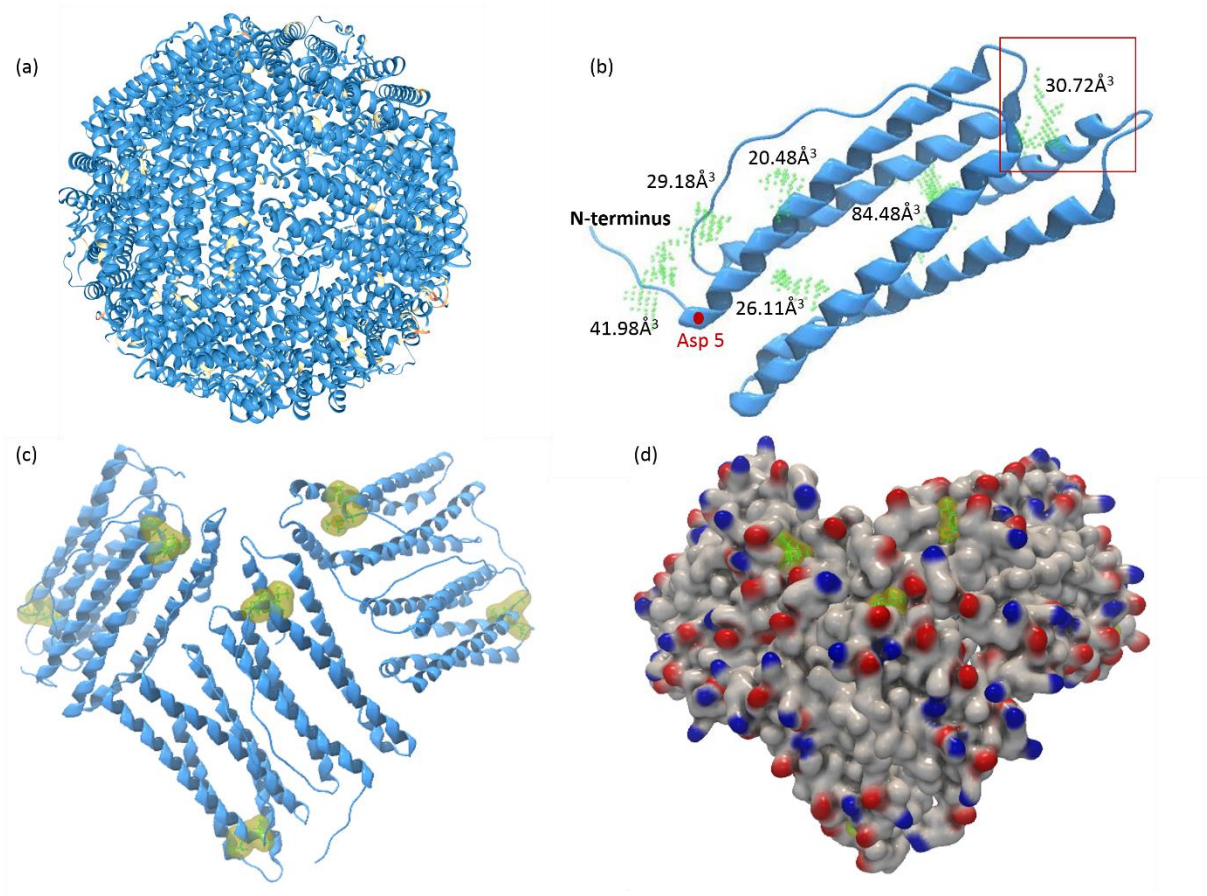

Figure 2. Different monomers of the 24-mer ferritin (a) The 24-subunit self-assembled ferritin (PDB: 3EGM). (b) Ferritin subunit showing six hydrophobic binding pockets (dotted green) of different sizes modelled using CLC Drug Discovery software. HA fused with the ferritin at Asp^5. Binding pocket 30.72Å^3 was selected for ligand docking because it was likely to be minimally influenced by HA attached to Asp^5. (c) Six subunits of ferritin (3EGM) illustrating the selected hydrophobic binding region (green) on the surface of the protein. (d) Surface display of the hydrophobic and hydrophilic residues on the ferritin. It can be observed that the selected binding regions (green) are on the surface and accessible for reversible binding with a target ligand.

Synthesis of Ligands Boc-SJ047 and Boc-SJ055. The design focused on simple glycine-dervied Ugi products SJ047 and SJ055 which have the amine available as a point of attachment for linking to the support. These glycine-derived Ugi products were easy to synthesise in solution (see supplementary information 1.0). Ligands Boc-SJ047 and Boc-SJ055 were synthesised in isolated yields ≥70%. In previous reports, the Ugi one-pot mixture of furfurylamine, benzaldehyde, boc-glycine and *tert*-butyl isocyanide resulted in an isolated

yield of 66%.[17] Moreover, Torroba and workers used cyclohexyl isocyanide in an Ugi reaction to achieve yields >80%.[18] To synthesise ligand Boc-SJ047, the *tert*-butyl isocyanide was substituted with cyclohexyl isocyanide, in an attempt to increase hydrophobicity for ferritin target region binding. This modification resulted in an increased yield of 95% for ligand Boc-SJ047.

Furthermore, for ligand Boc-SJ055, the benzaldehyde component was replaced by 2-pyridinecarboxaldehyde, to examine the effect of the change of its hydrophobicity on HA-Ferritin binding. 2-Pyridinecarboxaldehyde has been used previously in the Ugi reaction to synthesise α,β-unsaturated γ-lactams in good yields.[19] The second ligand Boc-SJ055 had an isolated yield of ~71%. Before synthesis of the affinity matrix, the ligands were deprotected to yield the amino compounds. 2D-NMR characterisation and mass spectrometry was carried out for both lead ligands (protected and deprotected analogues) to confirm the proposed structures.

Docking of ligand SJ047. The most accessible hydrophobic binding pocket (30.72 $Å^3$) was the most distant from the NH_2-terminus and the protruding HA spikes (Figure 3a). Ligand SJ047 was docked into the hydrophobic pocket of the most accessible ferritin subunit (Figure 3b) using CLC Drug Discovery Workbench. The highest docking score with the best possible orientation of interaction between ligand SJ047 and the protein was analysed. In addition to the suggested hydrophobic interactions with the ferritin residues, CLC simulated the formation of hydrogen bonds with glutamine, threonine and asparagine residues (Glu^{81}, Thr^{84} and Asn^{146}). Ligand SJ055 was docked in the same 30.72 $Å^3$ hydrophobic pocket in a different orientation from ligand SJ047 due to the substitution of the benzene with pyridine of ligand SJ055.

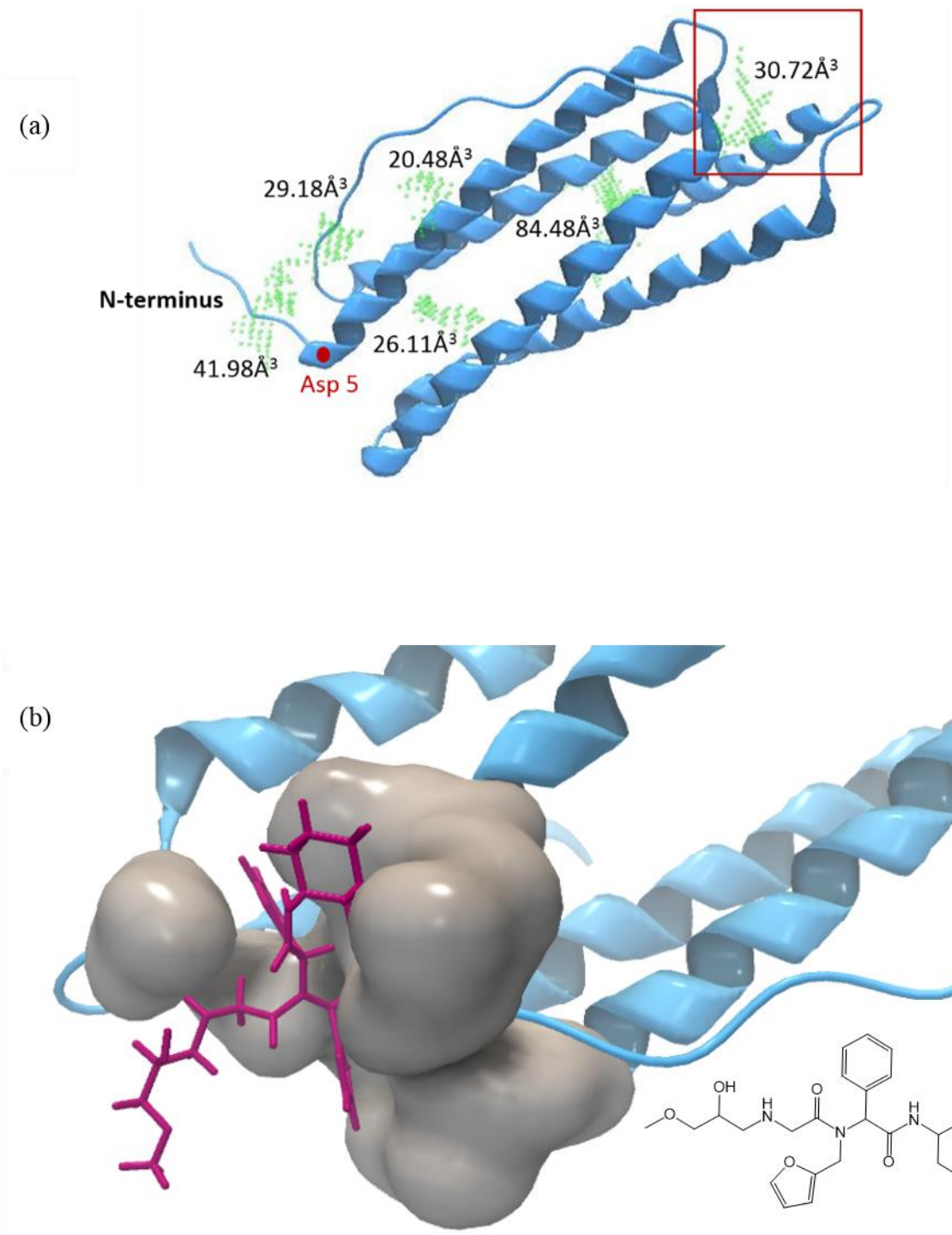

Figure 3. Molecular docking of ligand SJ047 into ferritin hydrophobic target site. (a) Ferritin subunit (PDB: 3EGM) showing six hydrophobic binding pockets of different sizes modelled using CLC Drug Discovery software. HA fused with the ferritin at Asp^5. Binding pocket 30.72$Å^3$ was selected for ligand docking because it was likely to be minimally influenced by HA attached to Asp^5. (b) Ligand SJ047 being docked into the hydrophobic pocket.

Immobilisation of fluorescent ligand SJ056. After NMR characterisation of the deprotected ligands, they were immobilised on the Sepharose CL-4B support. Before immobilisation, the method of coupling was assessed using a fluorescent ligand SJ056 (supplementary data 4.0) as a way of evaluating the reaction conditions required to immobilise the deprotected ligand to the epoxy activated resin. The ligand SJ056 was immobilised to the epoxy activated resin under alkaline conditions with the initial reaction of the epoxide with a primary amine producing a product containing a secondary amine and a secondary alcohol (Figure 4). The epoxide group reacts with the primary amine nucleophile in a ring-opening process.[20] As amine nucleophiles react at more moderate alkaline pH values of approximately 9,[21] triethylamine was added to maintain the alkaline pH and inhibit hydrolysis of the epoxide group. Once the ligand was immobilised the fluorescence was monitored using a fluorimeter and fluorescence microscopy.

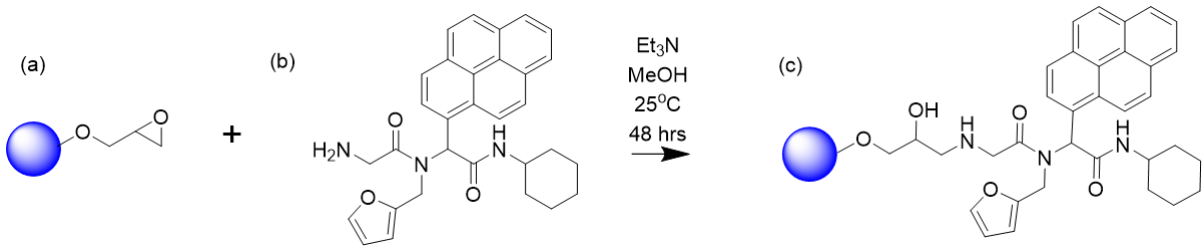

Figure 4. The reaction for the immobilisation of ligand SJ056 with the epoxy activated Sepharose beads. (a) Epoxy activated resin using epichlorohydrin spacer. (b) Fluorescent ligand SJ056, the ligand has a primary amine group exposed to react with the epoxide group in alkaline conditions. (c) The coupling of the ligand and resin produces a secondary amine and a secondary alcohol which is on the carbon ß to the carbon containing the amine nitrogen.

PEGDE 500 was immobilised to the resin, whence the fluorescent ligand SJ056 was coupled to the epoxy activated resin. Images of the unmodified Sepharose CL-4B and the resin coupled with fluorescent ligand SJ056 were captured using an Olympus CX40 microscope (Figure 5). Fluorescence studies were performed using a Nikon EFD-3 filter (λex = 330-380nm) to observe the immobilised fluorescent ligand.

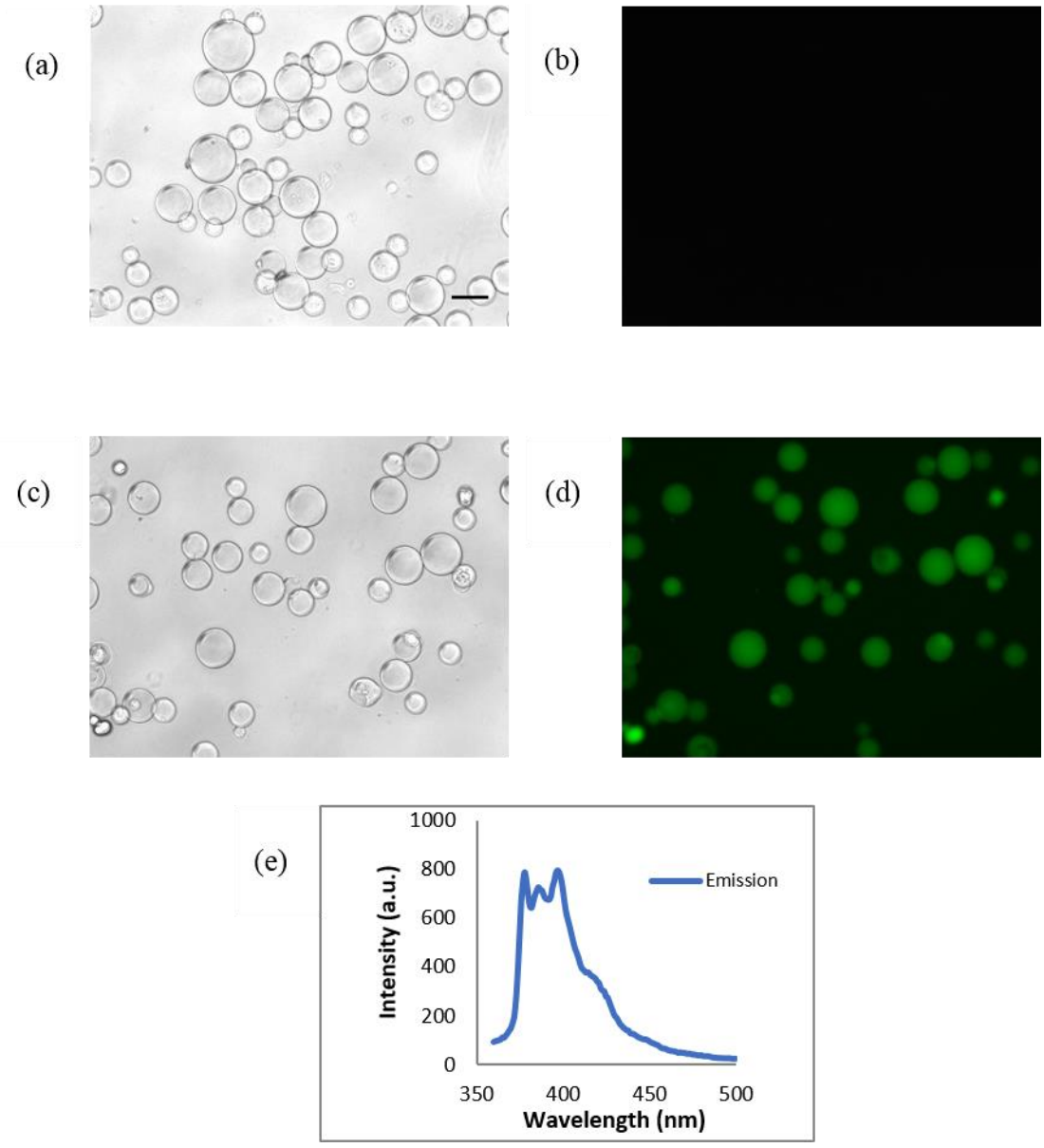

Figure 5. Immobilisation of fluorescent ligand SJ056. (a) Unmodified Sepharose CL-4B beads under visible light in methanol. (b) Unmodified Sepharose under Nikon EFP-3 filter in methanol. The scale bar represents 100µm. (c) Ligand SJ056 activated PEG-Sepharose beads under visible light in methanol. (d) Ligand SJ056 activated PEG-Sepharose beads under Nikon EFP-3 filter in methanol. (e) Emission spectrum of ligand SJ056 activated PEGDE-Sepharose in methanol measured using a fluorimeter.

Apparent dissociation constants of ligands SJ047 and SJ055 modified biosensor tips. The FortéBIO Octet system follows the Langmuir isotherm and thus the apparent dissociation constants can measured against ferritin. The instrument uses bio-layer interferometry to analyse the interference pattern of white light.[22] Analysis occurs on disposable fiber-optic biosensor tips in a "dip and read" manner using microtiter plates. The Ugi ligand activated biosensor tip bound ferritin and caused a shift in the interference pattern.[22] The wavelength shift was generated by the change in thickness of the bound ferritin layer, which then allowed real-time apparent dissociation constants to be measured. Furthermore, for the determination of kinetic rate constants there is evidence that the Octet generates kinetic binding constants comparable to other biosensor instruments used in industry.[23]

Both functionalised tips were tested against an increasing concentration of ferritin (0 to 1 mg/mL) in a step change and calibrated using a non-functionalised tip. The apparent K_d of ligands SJ047 and SJ055 were 2.04×10^{-7} M and 1.91×10^{-8} M, respectively (Figure 6). SJ055 demonstrated an almost 10-fold higher binding affinity compared to SJ047. The previously observed dissociation constant of an Ugi ligand against immunoglobulins was 2.6×10^{-6} M.[10] The previously measured apparent dissociation constant of immunoglobulins was determined on the Sepharose beads and the constant was determined indirectly using absorbance at 280 nm. In comparison, in this work, a more efficient method using bio-layer interferometry was used to determine the apparent dissociation constants for the ferritin-binding Ugi ligands. Nevertheless, ligand SJ047 and SJ055 displayed a high binding affinity when using the Octet, and were thus immobilised onto epoxy functionalised beads and screened for binding to purified ferritin.

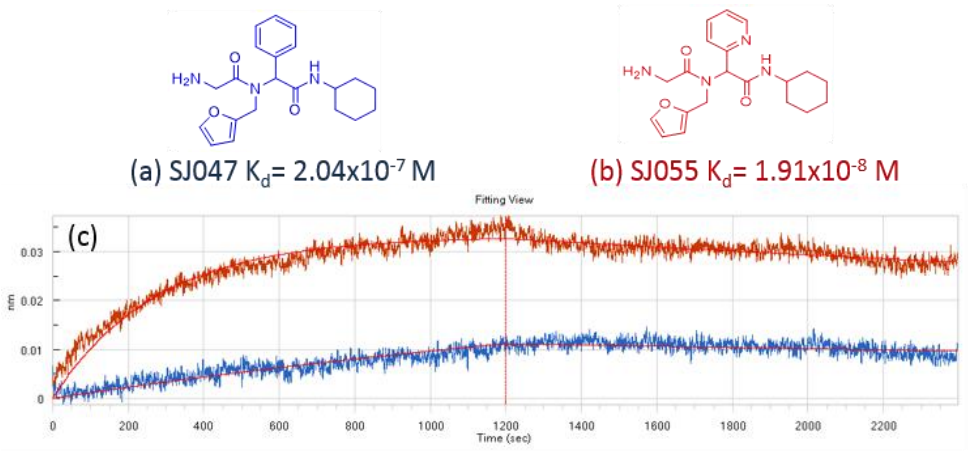

Figure 6. Apparent affinity constants of ligand SJ047 and SJ055. (a) Ligand SJ047 displaying apparent affinity constant against ferritin measured using the Octet RED96. (b) Ligand SJ055 displaying the apparent affinity constant against ferritin. c) The wavelength shift in nanometers against time in seconds (blue, SJ047; red, SJ055).

Control experiments. Control experiments were conducted to confirm that there were minimal non-specific interactions between the HEK crude supernatant and the unmodified Sepharose beads and between the PEG cis-diol functionalised Sepharose beads (see supplementary information, 5.0). It was observed that there was no significant binding between the unmodified Sepharose and the antigen and only weak binding was observed to the PEG cis-diol functionalised Sepharose even with relatively high salt concentrations in the binding buffer. From the HEK crude cell supernatant, the HCP impurities were identified by MALDI mass spectrometry to characterise the proteins (see supplementary information, 6.0).

Purification of HA-Ferritin spiked into HEK supernatant using SJ047-functionalised resin. Different concentrations of ammonium sulphate were tested with the binding buffer in order to find the conditions that the ligand SJ047-functionalised resin bound HA-ferritin only and removed the unbound HEK host cell protein impurities (HCP) in the flow through fractions. High ammonium sulphate (1.6 M) concentrations were trialled to promote hydrophobic interactions between the ligand and the recombinant antigen. However, both the recombinant antigen and the HCP impurities were bound and eluted. Therefore, the ammonium sulphate concentration in the binding buffer was reduced to 1.2 M and then subsequently to 1.08 M. For the purification of the three HA-ferritin strains, optimal binding was achieved at physiological pH 7 in 20 mM PIPES, 1.08 M ammonium sulphate and the optimal linear negative gradient elution in 20 mM PIPES, was found to be 1.08 M – 0.54 M ammonium sulphate. The HCP impurities were mainly observed in the flow through and wash fractions and the majority of the recombinant antigens were seen in the E2 and E3 fractions for all strains (Figure 7).

A decreased salt concentration was used to reduce the hydrophobic interactions[24] and promote other interactions such as hydrogen bonding between the ligand and the recombinant antigen. Therefore, this approach increases the probability of the ligand binding the ferritin hydrophobic pocket as the salt is sufficient to promote hydrophobic interactions and hydrogen bonding.

The ligand was tested against all three strains to test the optimised conditions. To achieve high purity and yield, fractions were combined (Table 1). HA (New Caledonia)-ferritin had the highest average purity and yield in lanes E2 to E4, 92.9±0.9% and 81±1%, respectively (Table 1). It was observed that lanes E2 to E4 contained the majority of the HA (New Caledonia)-ferritin, corresponding to ammonium sulphate concentration in the range 0.82 – 0.54M in the linear gradient (Figure 7a). In lanes E2 and E3, HA (California)-ferritin was the most concentrated with average purity and yield of 89.8±0.3% (n=2) and 71±0.8% (n=2),

respectively. The eluting ammonium sulphate concentration gradient fell from 0.82 M to 0.69 M in lanes E2 to E3 (Figure 7b). Lastly, HA (Singapore)-ferritin showed faintly on the gel as elution was spread across lanes E2 to E5, and these were calculated to have an average purity of ~75% and a yield of ~55%. The reduction in salt concentration across these lanes averaged from 0.82 M to 0.54 M, similar to HA (New Caledonia)-ferritin (Figure 7c). HA (Singapore)-ferritin requires further optimisation in order to achieve high purity and yield compared to the other two strains; however, the purification method proved successful across all three strains. The main reason for low purity and yield from the purification of HA (Singapore)-ferritin is due to the low expression levels compared to the other two strains; even though, 0.1 mg/mL of HA(Singapore)-ferritin was being added, the dilution rate was much higher as this was indicated by faint bands on the gel.

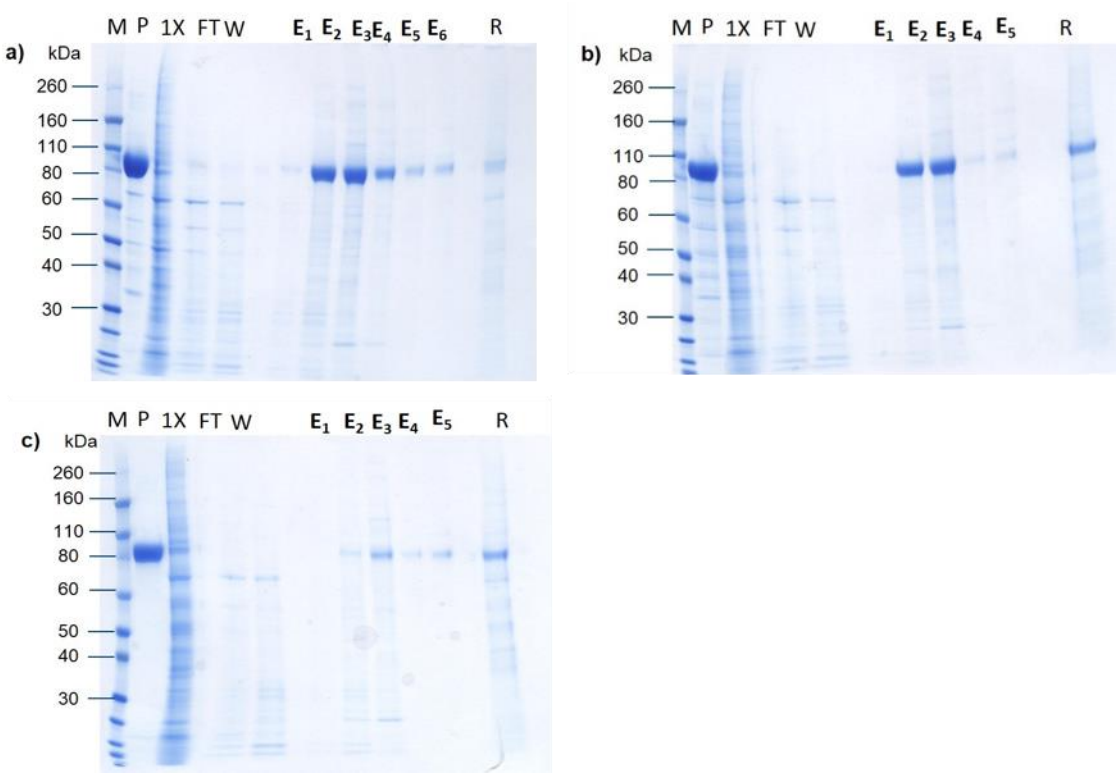

Figure 7. Purification of recombinant antigens using functionalised resin SJ047.Colloidal blue SDS-page of: (a) HA(New Caledonia)-ferritin spiked into 5X HEK supernatant loaded (0.1 mg/mL of resin) onto the ~1 mL ligand SJ047 packed column and purified on the ÄKTA avant (b) HA(California)-ferritin spiked into 5X HEK supernatant loaded onto ~1 mL ligand SJ047 packed column and purified. (c) HA(Singapore)-ferritin spiked into 5X HEK supernatant loaded onto ~1 mL ligand SJ047 packed column and purified. Legend for SDS-PAGE above, M: Marker (Pre-stained 10 kDa ladder), P: Purified HA-Ferritin (5 µg), 1X: 1X supernatant of HEK culture, FT: Column wash (20 mM PIPES, 1.08M $(NH_4)_2SO_4$), W: Column wash (20 mM PIPES, 1.08M $(NH_4)_2SO_4$), Ex: Gradient elution fraction to 20 mM PIPES, R: Regeneration fraction

Table 1. Yield and purity of combined lanes measured using densitometry analysis (ImageJ) for ligand SJ047.For HA (Singapore)-ferritin, the elution fractions E2-E5 for the repeated run were not very visible, therefore, the results of the first run are displayed. The standard error is reported for two repeated runs (n=2).

Antigen strain	Lanes (Salt, M)	Purity	Yield
HA (New Caledonia)–ferritin	E2-E4 (0.82-0.54)	92.9±0.9%	81±1%
HA (California)–ferritin	E2 & E3 (0.82-0.69)	89.8±0.3%	71±0.8%
HA (Singapore)–ferritin	E2-E5 (0.82-0.54)	~75%	~55%

Purification of HA-Ferritin spiked into HEK supernatant using SJ055-functionalised resin. As with the SJ047-functionalised resin, different ammonium sulphate concentrations to the binding and elution buffers were also explored for purifying the expressed antigens with the SJ055-functionalised resin. For the purification of the three HA-ferritin strains, optimal binding was achieved at physiological pH 7 in 20 mM PIPES, 1.2 M ammonium sulphate and optimal linear negative gradient elution starting at 1.2 M ammonium sulphate and ending at 0.6 M ammonium sulphate. Compared to ligand SJ047, when 20 mM PIPES and 1.08 M ammonium sulphate concentration was trialled as a binding buffer with ligand SJ055, the recombinant antigen was observed in the flow through and wash fractions; therefore, 1.2M ammonium sulphate was used as the optimised buffer. As mentioned previously, this was due to ligand SJ055 being less hydrophobic than SJ047, and thus requiring more ammonium sulphate for adsorption. The disadvantage of using an increased salt concentration is that it results in lowered protein solubility and increased hydrophobic interactions, and thus promotes non-specific interactions between the ligand and the HCP impurities.

As previously, following the combination of the fractions, the purity and yield were determined (Table 2). HA (New Caledonia)-ferritin had the highest average purity and yield in lanes E2 to E4, 88.8±2.2% (n=2) and 72.5±0.5% (n=2), respectively (Table 2). It can be observed that lanes E2 to E4 had the majority of the HA (New Caledonia)-ferritin, corresponding to 0.91 M ammonium sulphate falling to 0.6 M in the linear gradient (Figure 8a). In lanes E2 and E3, HA (California)-ferritin was the most concentrated, with average purity and yield of 81±0.5% (n=2) and ~74±1% (n=2), respectively. The elution ammonium sulphate concentration gradient reduced from 0.91 M to 0.77 M in lanes E2 to E3 (Figure 8b). Lastly, HA (Singapore)-ferritin showed faintly on the gel and when the elution lanes E2 and E3 were selected, an average purity of ~87% and yield of ~78% were observed. The reduction in salt concentration across these lanes averaged 0.91 M to 0.77 M, similar to the HA (New Caledonia)-ferritin (Figure 8c).

Compared to ligand SJ047, apart from the increased salt concentration used, the purity and yield were reasonably comparable. For HA (New Caledonia)-ferritin, the yield was lowered from 81±1% (n=2) for ligand SJ047 to 72.5±0.5% (n=2) for SJ055, or HA (California)-ferritin the purity was lowered from 89.8±0.3% (n=2) for ligand SJ047 to 81±0.5% (n=2) for SJ055; however, for HA (Singapore)-ferritin, the yield and purity were much higher from ~75% for ligand SJ047 to 87% for SJ055 and ~55% for ligand SJ047 to 75% for SJ055, respectively. Therefore, both ligand adsorbents could potentially be used for the purification of HA-ferritin strains, however, if the presence of salt was a concern, immobilised ligand SJ047 would be the preferred resin.

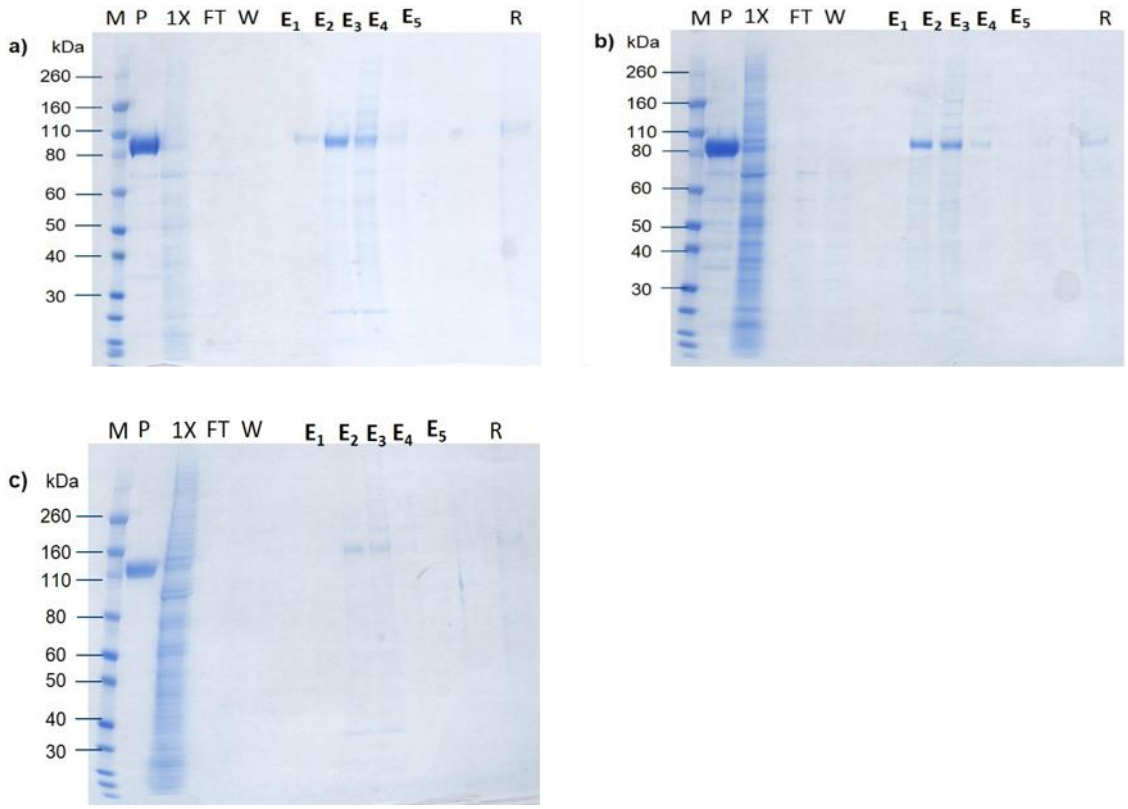

Figure 8. Purification of recombinant antigens using functionalised resin SJ055. Colloidal blue SDS-page of: (a) HA(New Caledonia)-ferritin spiked into 5X HEK supernatant loaded (0.1 mg/mL of resin) onto the ~1 mL ligand SJ055 packed column and purified on the ÄKTA avant (b) HA(California)-ferritin spiked into 5X HEK supernatant loaded onto ~1 mL ligand SJ055 packed column and purified. (c) HA(Singapore)-ferritin spiked into 5X HEK supernatant loaded onto ~1 mL ligand SJ055 packed column and purified.Legend for SDS-PAGE above, M: Marker (Pre-stained 10 kDa ladder), P: Purified HA-Ferritin (5 µg), 1X: 1X supernatant of HEK culture, FT: Column wash (20 mM PIPES, 1.2 M $(NH_4)_2SO_4$), W: Column wash (20 mM PIPES, 1.2 M $(NH_4)_2SO_4$), E_X: Gradient elution fraction to 20 mM PIPES, R: Regeneration fraction

Table 2. Yield and purity of combined lanes measured using densitometry analysis (ImageJ) for ligand SJ055. For HA (Singapore)-ferritin, the elution fractions E2-E5 for the repeated run were not very visible, therefore, the results of the first run are displayed. The standard error is reported for two repeated runs (n=2).

Antigen strain	Lanes (Salt, M)	Purity	Yield
HA (New Caledonia)–ferritin	E2-E4 (0.91-0.6)	88.8±2.2%	72.5±0.5%
HA (California)–ferritin	E2 & E3 (0.91-0.77)	81±0.5%	74±1%
HA (Singapore)–ferritin	E2 & E3 (0.91-0.77)	~87%	~78%

Purification of HA-Ferritin from crude mixture using Ugi functionalised resins. As in the case of the spiked artificial supernatant, different ammonium sulphate concentrations were also trialled in order to find optimal binding conditions for the crude HEK expressed recombinant antigen on the ligand SJ047 and SJ055-functionalised resins. Below salt binding conditions containing 1.6M ammonium sulphate, the recombinant antigen was observed in the flow through and wash fractions. However, at this elevated salt condition, some of the HCP impurities were bound and eluted in the gradient elution. As mentioned previously, increased ammonium sulphate concentrations may reduce protein stability. Since proteins show a sharp fall in solubility with increasing salt concentration beyond a particular threshold causing the proteins to precipitate or 'salt out'.[25] In addition, impurities can also 'salt out' with the target protein.[26]

Nevertheless, purification was carried out using the binding buffer 20 mM PIPES containing 1.6 M ammonium sulphate with negative gradient elution reducing the 1.6 M ammonium sulphate concentration to 0.6 M. For both ligand resins, elution of the recombinant antigen was observed in lanes E2 to E6; however, some of the characterised HCP impurities were seen in lanes E2 and E3 (Figure 9). The previous control experiments suggested that there might be binding between the PEG spacer and the impurities.

As previously mentioned, to achieve high purity and yield, fractions were combined (Table 3). For ligand SJ047, HA (New Caledonia)-ferritin showed an average purity and yield from combined lanes (E2 to E5) of 85±0.5% (n=2) and ~97±1% (n=2), respectively (Table 3). Elution lanes E2 to E5 contained the majority of the HA (New Caledonia)-ferritin, corresponding to ammonium sulphate in the range of 1.22 – 0.8 M in the linear gradient (Figure 9a). For ligand SJ055, HA (Caledonia)-ferritin was the most concentrated with average purity and yield of 87.5±0.5% (n=2) and 95.5±1.5% (n=2), respectively, from lanes E2 to E6. Similarly, the elution occurred at an ammonium sulphate concentration within the range 1.22 -

0.8 M from lanes E2 to E6 (Figure 9b). Both ligands were comparable and conditions could be further optimised to achieve a higher purity. The purification method at an automated 1 mL scale was shown to be successful against the crude sample.

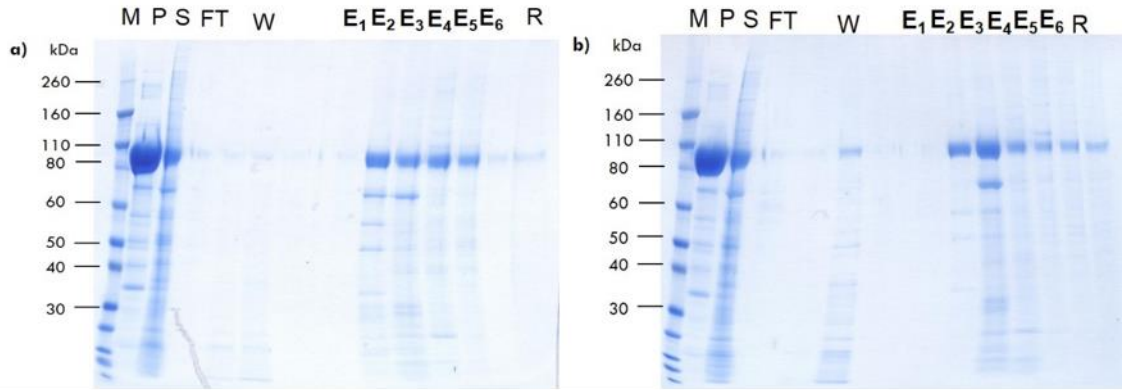

Figure 9. Purification of HEK expressed HA (New Caledonia)-ferritin using functionalised resins SJ047 and SJ055. Colloidal blue SDS-page of: (a) Clarified HEK expressed HA(New Caledonia)-ferritin supernatant (0.1 mg/mL of resin) onto the ~1 mL ligand SJ047 packed column and purified on the ÄKTA avant (b) Clarified HEK expressed HA(New Caledonia)-ferritin supernatant (0.1 mg/mL of resin) loaded onto ~1 mL ligand SJ055 packed column and purified. Legend for SDS-PAGE above, M: Marker (Pre-stained 10 kDa ladder), P: Purified HA(New Caledonia)-Ferritin (5 µg), 1X: 1X supernatant of HEK culture, FT: Column wash (20 mM PIPES, 1.6 M $(NH_4)_2SO_4$), W: Column wash (20 mM PIPES, 1.6 M $(NH_4)_2SO_4$), E_X: Gradient elution fraction to 20 mM PIPES, R: Regeneration fraction

Table 3. Yield and purity of combined lanes measured using densitometry analysis (ImageJ) for ligands SJ047 and SJ055. The standard error is reported for two repeated runs (n=2).

Antigen strain	Ligand	Lanes (Salt, M)	Purity	Yield
HA (New Caledonia)–ferritin	SJ047	E2-E5 (1.22-0.8)	85±0.5%	97±1%
HA (New Caledonia)–ferritin	SJ055	E2-E6 (1.22-0.8)	87.5±0.5%	95.5±1.5%

Capacity Studies of HA (NC)-Ferritin from HEK cell supernatants. Increasing concentrations of HA (NC)-Ferritin were purified to evaluate the capacity of the functionalised resin column (Table 4). Both the increase in wash buffer ammonium sulphate concentrations (1.08 M to 1.6 M) and increasing load of HA (NC)-ferritin were tested to evaluate the maximum capacity of the amount of antigen that can be retained before breakthrough is observed in the flow through and wash fractions (see supplementary information, 7.0).

Due to the increase in the total amount of protein load on the column (antigen and HCP impurities amount), a higher ammonium sulphate concentration was needed to purify the crude cell supernatant and retain the antigen. Therefore, the maximum capacity was achieved with 1.6M ammonium sulphate as the wash buffer, however, both functionalised columns were able to achieve 0.1mg/mL of capacity. For the SJ047-functionalised column, at 0.25 mg/mL load, HA(NC)-ferritin was being purified, however >30% of the antigen was being observed in the flow through and wash fractions (Figure S6). For the SJ055-functionalised column, 0.25 mg/mL load, HA(NC)-ferritin was not being purified to the same level and >50% of the antigen was being observed in the flow through and wash fractions. The difference in purification, is due to the fact that ligand SJ055 is more hydrophilic and requires a higher salt concentration to adsorb the antigen.

Overall, the main reason for such low capacity is due to the size of the column. In such an increasing load of total protein, the column capacity was not sufficient as the target binding sites of the ligand are saturated with the antigen. Therefore, to retain the maximum amount of antigen the salt concentration was increased, however, this enhanced non-specific binding of the target ligand to the HCP impurities. Nevertheless, to overcome these issues the column size could be scaled up, and as a result less salt used in the binding buffer. Furthermore, other solid supports (membrane cellulosic filters) that have greater capacity and overcome diffusional limitations could be employed.

Table 4. Maximum binding capacity of HA(NC)-Ferritin, observed through SDS-PAGE (see supplementary information, 7.0). The sample HA (NC)-Ferritin from HEK cell supernatants was added in increasing concentration to be purified by the ~1 mL SJ047 and SJ055 funtionalised columns. The fractions were collected and the purification was analysed using SDS-PAGE (Commassie stain). Breakthrough of HA (NC)-ferritin was observed by checking the flow through (FT) and wash (W) fraction on the SDS-PAGE for the presence of HA-Ferritin. Different salt concentrations were also tested to find the optimal concentration where the maximum binding capacity of HA-ferritin can be achieved.

	HA(NC)-ferritin Loaded mg/mL of resin :	**0.05**	**0.1**	**0.25**	**0.42**	**1.7**
Wash buffer (20 mM Pipes + X salt concentration (M))	Ligand	Breakthrough seen in FT & W fractions (Yes/No)				
1.08	SJ047	-	Y	-	Y	Y
1.2	SJ047	-	Y	-	-	-
1.6	SJ047	N	N	Y	-	-
1.08	SJ055	-	Y	-	-	-
1.2	SJ055	-	Y	-	-	-
1.6	SJ055	-	N	Y	-	-

Structural integrity of recombinant antigens. Structural studies of the eluted recombinant antigens was carried out from both the artificial mixture and the HEK expressed HA (New Caledonia)-ferritin supernatant. After purification, it is vital to assess the structural integrity of these large (~2000 kDa) recombinant HA-ferritin (diameter: ~40 nm) as they are exposed to high salt concentrations, shear and different buffered conditions. Therefore, the elution fractions of the recombinant antigen strains were tested for aggregation using dynamic light scattering (DLS) and absorbance at 350 nm.

Absorbance (λ = 350 nm). After automated purification, the integrity of the HA (New Caledonia)-ferritin was assessed as the ammonium sulphate concentration was high. Therefore, the recombinant antigen was tested for the formation of aggregates through using absorbance measurements. The absorbance at $\lambda = 350$ nm is a measure of the turbidity and hence is a

quantitative measure of the aggregation process.[27] An experiment was conducted where 100 µg/mL of HA (New Caledonia)-ferritin was buffer exchanged with 20 mM PIPES and 1.6M ammonium sulphate, agitated and measured for absorbance at 350 nm every hour for 5 hours. All readings were very similar and close to zero suggesting that the recombinant antigen showed no signs of aggregation.

Dynamic light scattering (DLS). DLS is used to determine the size distribution profile of small particles in solution. DLS uses the principles of Brownian motion and Doppler shift to determine the hydrodynamic size and number of particles in a suspension.[28] In this instance, the elution fractions were evaluated for the hydrodynamic diameter of the HA-ferritin strains. The expected diameter is ~35-45 nm for HA-ferritin strains,[5] Table 5 below demonstrates the hydrodynamic diameter achieved after purification of both the artificial mixture and HEK expressed HA (New Caledonia)-ferritin supernatant using functionalised resins SJ047 and SJ055.

The hydrodynamic diameter results for the purification of the artificial mixture had one anomalous result; 59.0 nm diameter of HA (New Caledonia)-ferritin purified by SJ055. This result could be due to the polydispersity of the sample; thus, this strain could be aggregating. Nevertheless, for the purification of the artificial mixture using functionalised resins SJ047 and SJ055, the range of hydrodynamic diameters were from 33.1-34.9 nm, within the range of expected approximate hydrodynamic diameters. Moreover, after HEK expressed HA (New Caledonia)-ferritin supernatant purification using functionalised resins SJ047 and SJ055; the hydrodynamic diameters achieved were 44.8 nm and 39 nm, respectively. The size distribution confirms the majority presence of the stable recombinant HA (New Caledonia)-ferritin antigen after purification using the functionalised resins SJ047 and SJ055 (Figure 10). Further studies can be carried out to assess the activity of the haemagglutinin through haemagglutinin

inhibition (HI) assay.[5] However, this assay does not consider the structural integrity of the recombinant antigens.

Table 5. The hydrodynamic diameter achieved after purification using functionalised resins SJ047 and SJ055. Elution fractions E2 and E3 were assessed and the omitted results did not have sufficient protein volume that can be analysed.

Supernatant	Strain	Ligand used	Hydrodynamic diameter (nm)
HEK (5X) added	HA (New Caledonia) – ferritin	SJ047	34.9
	HA (California) –ferritin	SJ047	-
	HA (Singapore) –ferritin	SJ047	33.1
	HA (New Caledonia) – ferritin	SJ055	59.0
	HA (California) –ferritin	SJ055	34.5
	HA (Singapore) –ferritin	SJ055	-
HEK expressed	HA (New Caledonia) – ferritin	SJ047	44.8
	HA (New Caledonia) – ferritin	SJ055	39.0

(a)

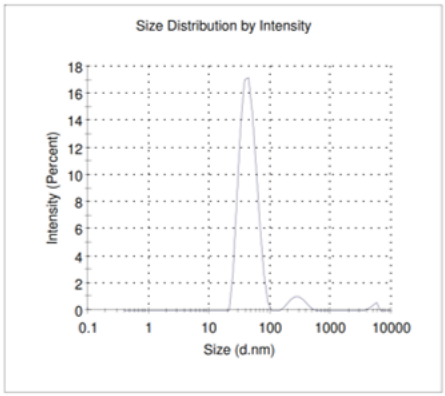

(b)

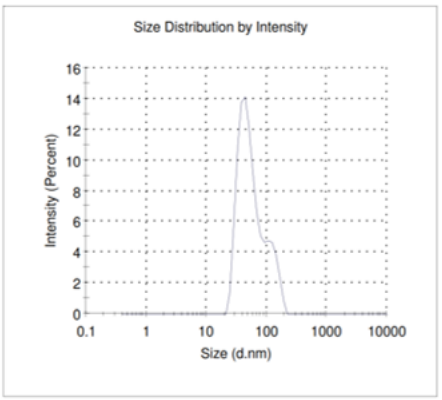

Figure 10. DLS Size distribution by intensity of: (a) Purified HA (New Caledonia)-ferritin by functionalised resin SJ047 from HEK expression. Hydrodynamic diameter of purified HA (New Caledonia)-ferritin is 44.8 nm. (b) Purified HA (New Caledonia)-ferritin by functionalised resin SJ055 from HEK expression. Hydrodynamic diameter of purified HA (New Caledonia)-ferritin is 39.0 nm.

Conclusions

Influenza is a serious threat to public health; hence, there is a large market for vaccines. Typically, hen's eggs are used for upstream processing of the virus, although manufacturing innovations are moving towards using recombinant DNA technology to produce the antigens as this is time and cost effective.[5] Novel self-assembling recombinant antigens have been shown to lead to broader and more potent protection. Furthermore, the combination of the universal ferritin core and the development of synthetic affinity ligands offers an ideal platform for affinity chromatography as a universal purification method. The final purities achieved with the lead ligands were comparable to the purities achieved after other multiple step purification methods. This suggested that, with more development, this methodology could be a contender in the development of an efficient and cost-effective influenza antigen purification protocol.

Experimental Procedures

General material and methods. Recombinant protein purification was carried out using the ÄKTA avant (GE Healthcare, Uppsala, Sweden). Dynamic light scattering studies were carried using Malvern Instruments Zetasizer Nani series Nano S. SDS-PAGE gels were run using a Novex® Mini-Cell gel tank (Bio-Rad, USA), scanned using HP Scanjet 5530 photosmart scanner and analysed with Image J. For the organic synthesis of Ugi ligands, all reactions were carried out in oven-dried glassware under a nitrogen atmosphere unless otherwise indicated. An Olympus CX40 microscope and a Varian eclipse fluorescence spectrophotometer (fluorimeter) were used for the fluorescence studies. CEM Discover microwave reactor was used for the synthesis of Ugi ligands. ^{1}H NMR, ^{13}C NMR, and 2D-NMR spectra were recorded at 400 MHz on a Bruker Avance 400 spectrometer. Mass spectra were obtained using Waters LCT Premier mass spectrometer at the Department of Chemistry, University of Cambridge.

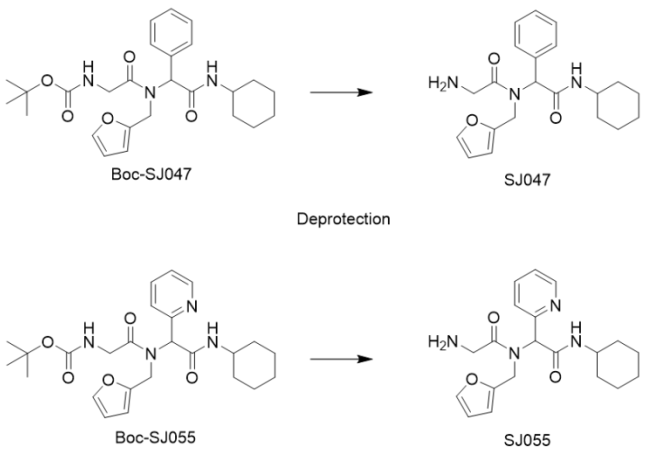

Figure 11. Boc-protected and deprotected ligands SJ047 and SJ055.

Docking of ligand SJ047. Ferritin (PDB:3EGM) was imported into CLC Drug Discovery software and using the find binding pocket tool/algorithm, the six different putative binding pockets were identified. In the project tree, the binding pocket furthest away from the N terminus (30.72 $Å^3$) was selected. In the side panel, binding site setup was initiated around the binding pocket.

Next, ligand SJ047 was constructed in ChemDraw and saved as a SMILES (simplified molecular-input line-entry system) string which was imported into the CLC drug discovery software as a small molecule. Below the project tree, the dock ligand button imports the ligand into the binding pocket and carries out algorithms that inspect the docking result. A particular binding mode of a ligand in the protein binding pocket is connected with a score.

The molecular docking simulation searched through numerous potential binding modes of the ligand in the pocket, and the one resulting in the best score is returned from the docking. The best conformation and score of ligand SJ047 interacting with the ferritin binding pocket are shown in Figure 2. In addition, this docking method was carried out for ligand SJ055 before beginning *in vitro* testing.

Boc-SJ047,*tert*-butyl(2-((2-(cyclohexylamino)-2-oxo-1-phenylethyl)(furan-2ylmethyl)amino)-2-oxoethyl)carbamate.

Furfurylamine (376µL, 4.25 mmol) was dissolved in 0.8 mL of methanol a solution of benzaldehyde (435µL, 4.25mmol) 0.8 mL of methanol was added. The solution was stirred for 1.5 h, and imine formation was monitored using ^{1}H NMR (400 MHz). Subsequently, Boc-glycine (0.75g, 4.25mmol) and cyclohexyl isocyanide (530µL, 4.25mmol) were dissolved in 0.8 mL of methanol each and added to the reaction. The reaction was monitored using thin layer chromatography (TLC) and ^{1}H NMR. A white precipitate was observed and it was purified using column chromatography in silica gel. A ratio of petroleum ether and ethyl

acetate, 70:30 (v/v) to 0:100 (v/v) step wise, respectively were used to purify the Ugi component. White solid. Yield 95%. ^{1}H NMR (400 MHz, $CDCl_3$) δ 7.31-7.28 (m, 5H, H_a), 7.24 (d,1H, J=1.1 Hz, H_{b*}), 6.15 (s, 1H,H_{b1}), 5.90 (s,1H, H_c), 5.73 (s,1H,H_{b2}), 5.49 (s, 1H, H_d), 4.52 (d,1H,J=17.8 Hz, H_e), 4.50 (d,1H,J=17.8 Hz, H_e), 4.21 (s, 2H, H_f), 3.81 (tq, 1H,J=11.2, 3.8 Hz, H_g), 1.96-1.86 (m, 2H, H_h), 1.73-1.58 (m, 3H, H_h) 1.47 (s, 9H, H_i), 1.42-1.28 (m, 2H, H_h), 1.19-1.05 (m, 3H, H_h). ^{13}C NMR (400 MHz, $CDCl_3$) 155.7, 142.1, 134.4, 129.6, 128.7, 128.6, 110.5, 108.0, 79.6, 64.1, 63.1, 48.7, 42.9, 42.6, 32.8, 28.4, 25. 5, 24.8, 24.7. LRMS (ES+) 470 (M+H). HRMS (ES+) calculated for "$C_{26}H_{36}O_5N_3$" 470.2649 (M+H), found 470.2632.

Deprotected SJ047, 2-amino-N-(2-(cyclohexylamino)-2-oxo-1-phenylethyl)-N-(furan-2-ylmethyl)acetamide.

The general procedure for the deprotection of the Boc-group was followed for all Boc-protected Ugi ligands.[29] Once deprotected (Figure 11), dichloromethane (10 mL) was added to the TFA salt and the contents were then transferred to a separating funnel and 10 mL of 10% sodium hydroxide solution (w/v), mixed well, and the organic layer was separated. The remaining free amine was extracted into the organic layer. Then, the organic layers were combined, washed with water (10mL) and dried over anhydrous magnesium sulphate. The magnesium sulphate was removed under filtration and the organic layer concentrated *in vacuo*. The Boc-deprotected free-amine ligand was analysed by 2D-NMR and mass spectrometry. White solid. Yield 64%. ^{1}H NMR (400 MHz, $CDCl_3$) δ 7.42-7.29 (m, 5H, H_a), 7.22 (s,1H, H_{b*}), 6.14 (s, 1H,H_{b1}), 5.9 (s,1H, H_c), 5.74 (s,1H,H_{b2}), 5.63 (s, 1H, H_i), 4.5 (s, 2H, H_f), 3.82-3.78 (m, 1H, H_g), 3.68 (s,2H, H_e), 2.13 (s, 2H, H_d), 1.90-1.06 (m, 10H, H_h). ^{13}C NMR (400 MHz, $CDCl_3$) 168.5, 161.4, 141.7, 134.9, 129.6, 129.3, 128.7, 128.6, 126.5, 110.5, 108.6, 62.7, 48.6, 43.9, 42.2, 32.8, 25.5, 24.8, 24.7. LRMS (ES+) 370 (M+H). HRMS (ES+) calculated for "$C_{21}H_{28}O_3N_3$" 370.2125 (M+H), found 370.211

Boc-SJ055,tert-butyl(2-((2-(cyclohexylamino)-2-oxo-1-(pyridin-2-yl)ethyl)(furan-2 ylmethyl)amino)-2-oxoethyl)carbamate.

Boc-SJ055 (Figure 11) was synthesised using the same method as Boc-SJ047. However, the amount added and the concentration for each of the components were as follows: 2-pyrdine carboxaldehyde (202 µL, 2.12 mmol), furfurylamine (188 µL, 2.12 mmol), Boc-glycine (0.37g, 2.12 mmol), and cyclohexyl isocyanide (264 µL, 2.12 mmol). Yellow oil. Yield 71%. ^{1}H NMR (400 MHz, $CDCl_3$) δ 8.52 (s, 1H, H_{a*}), 7.64-7.60 (m, 1H, H_a), 7.52 (s, 1H, H_d), 7.30-7.24 (m, 2H, H_a), 7.21-7.19 (m, 1H, H_{b*}), 6.19 (s, 1H,H_{b1}), 6.0 (s,1H, H_c), 5.77 (s,1H,H_{b2}), 5.48 (s, 1H, H_{d*}), 4.71 (d, J=16.9 Hz, 1H, H_e), 4.66 (d, J=16.9 Hz, 1H, H_e)4.26 (s, 2H, H_f), 3.88-3.79 (m, 1H, H_g), 1.95-1.85 (m, 2H, H_h), 1.73-1.57 (m, 3H, H_h), 1.46 (s, 9H, H_i), 1.44-1.33 (m, 2H, H_h), 1.30-1.13 (m, 3H, H_h).

Deprotected SJ055, 2-amino-N-(2-(cyclohexylamino)-2-oxo-1-(pyridin-2-yl)ethyl)-N-(furan-2-ylmethyl)acetamide.

As for SJ047, the general procedure for the deprotection (Figure 11) of the Boc-group was followed.[29] Yellow solid. Yield 62%. ^{1}H NMR (400 MHz, $CDCl_3$) δ 8.58 (d, 1H, J=4.19, H_{a2}) , 7.72 (td, 1H, J=7.7, 1.7 Hz, H_a), 7.6-7.5 (m,1H, H_{a1}), 7.29-7.28 (m,1H,H_{a*}), 7.19 (s, 1H, H_{b*}), 6.3 (dd, J=3.2, 1.7 Hz, 1H, H_{b1}), 6.24 (d, J=3.2 Hz, 1H, H_{b2}), 6.18 (s, 1H, H_{d*}), 5.86 (s,1H, H_c), 5.20 (d, J=15.6 Hz, 1H, H_f), 4.52 (d, J=16.8 Hz, 1H, H_e), 4.03 (d, J=16.8 Hz, 1H, H_e), 3.82 (d, J=15.6 Hz, 1H, H_f), 3.87-3.82 (m, 1H, H_g), 1.87 (s, 2H, H_d), 1.72-1.11 (m, 10H, H_h). ^{13}C NMR (400 MHz, $CDCl_3$) 166.5, 165.5, 154.9, 150.2, 148.8, 148.4, 143.0, 137.1, 123.7, 123.5, 110.5, 110.0, 64.5, 45.6, 40.4, 36.2, 32.8, 32.7, 25.6, 25.1, 24.6. LRMS (ES+) 371 (M+H). HRMS (ES+) calculated for "$C_{20}H_{27}O_3N_4$" 371.2078 (M+H), found 371.2068.

Apparent dissociation constants using the fortéBIO Octet system. Apparent dissociation constants of the ligands interacting with ferritin were calculated using the Octet instrument. Firstly, the biosensor sensor tips were NHS ester activated following the method outlined in their AR2G manual and then deprotected primary amine ligands SJ047 and SJ055 were immobilised onto different tips. A blank tip was introduced as a negative control. Subsequently, an increasing concentration of ferritin from 0 to 1mg/mL was introduced and kinetic measurements were analysed by the Octet instrument.

The 'Amine Reactive Second Generation (AR2G)' carboxylic acid tip was firstly NHS ester (*N*-hydroxysulfosuccinimide) activated, whence the primary amine ligand reacted rapidly with the ester to form a ligand activated tip (Figure 12). The activation kit was obtained from Pall Life Sciences and the method was followed for NHS ester activation. The ligand was immobilised at physiological pH using HEPES buffered saline (HBS). After activation, the kinetics of association and dissociation between the immobilised ligand and ferritin were measured. The detailed protocol of the AR2G and Octet instrument manual were followed in order to obtain the apparent dissociation constant.

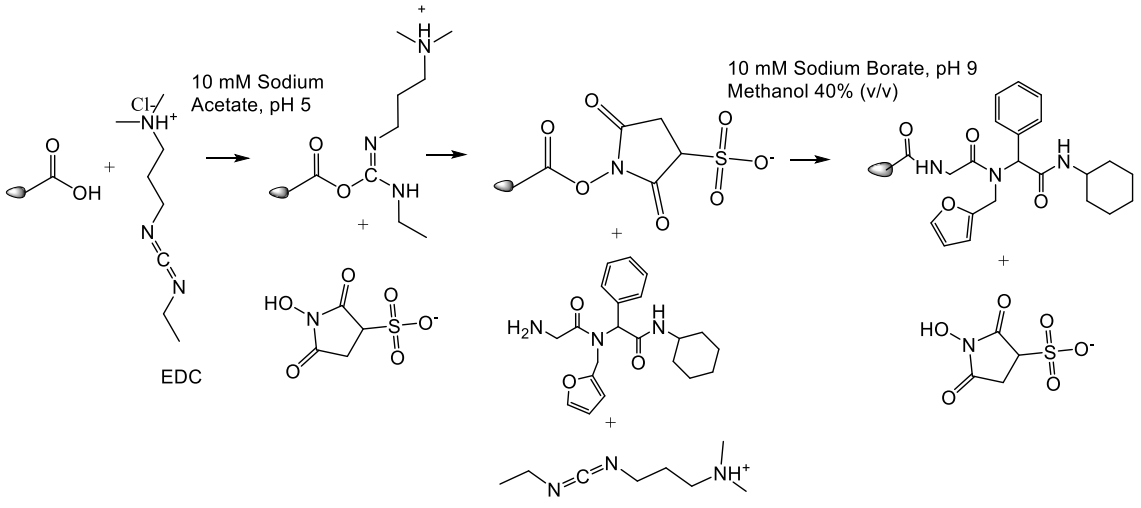

Figure 12. Covalent immobilisation of ligand on the AR2G biosensor. The carboxylic acid was activated by a reaction with EDC (1-Ethyl-3-[3-dimethylaminopropyl] carbodimide hydrochloride) and s-NHS (*N*-hydroxysulfosuccinimide). The ligand was dissolved in 40 % (v/v) methanol and 10 mM sodium borate and coupled with the NHS ester tip.

Synthesis of affinity matrix. The epoxide activation synthetic procedure and data was adopted from previous literature.[30] Sepharose CL-4B beads (2.5 g) were washed with UHP water on a glass filter-funnel and then mixed with 2M PEGDGE-500 (2.5 mL) and 0.6 M sodium hydroxide solution containing 2 mg mL^{-1} sodium borohydride (2.5 mL). The suspension was mixed by rotation (10 h, 30 °C), and the reaction was stopped by washing the gel on a glass filter-funnel with 5 mL of UHP water. The activated epoxide concentration was measured through titration with sodium thiosulphate; an activated resin of ~16.0 µmol epoxy groups g^{-1} moist weight was obtained.[30] ~60 mg–80 mg (4X molar excess) of the ligands was dissolved in methanol (2.5 mL) and triethylamine (~4 µL) was added. This was mixed with PEG-epoxy activated CL-4B beads (2.5 g) and left for 16 h at 30 °C. It was then washed 3 times with methanol (2.5 mL) and twice with 20% (v/v) of ethanol (2.5 mL). The beads were then packed into the column.

Acknowledgements

The authors would like to thank the Vaccine Production Program Laboratory, National Institutes of Health for providing financial support and providing the recombinant antigens for this work, special thanks to Dr. Masaru Kanekiyo, Dr. Diane Wycuff, Dr. Mridul Ghosh and Dr. Richard Schwartz. I would like to acknowledge and thank the Bampos Group, Department of Chemistry, Cambridge, Dr. Katherine Stott, Biophysics facility, Cambridge, and the Sheppard Group, Department of Chemistry, University College London (UCL) for their expertise. Dr. Laure Benhamou, Dr. Vincent Gray and Dr. Tom Sheppard for their support at UCL. In addition, thanks to the referees for their insightful and useful comments. Lastly, the guidance from Professor Christopher Lowe, Dr. Srishti Gupta, Dr. Basmah Khogeer, Dr. Graham Christie and Dr. Nick Bampos at the University of Cambridge has been very valuable.

Conflict of interest

The authors declare no financial or commercial conflict of interest.

Supporting information

Supporting information available contains characterisation of Ugi ligands using 2D-NMR spectroscopy and mass spectrometry. In addition, supporting data of the optical density experiments for the stability of HA (NC)-ferritin, control experiments and capacity measurements of the functionalised resins are included.

Abbreviation

Haemagglutinin-Ferritin (HA-Ferritin)

References

1. Mills, C. E., Robins, J. M., Lipsitch, M. (2004) Transmissibility of 1918 pandemic influenza. *Nature 432* (7019), 904-906.
2. Gerdil, C., The annual production cycle for influenza vaccine (2003). *Vaccine 21* (16), 1776-1779.
3. Tirrel, M. (2015), The $1.6 billion business of flu. http://www.cnbc.com/2015/10/19/the-16-billion-business-of-flu.html (accessed January 7th).
4. Besnard, L., Fabre, V., Fettig, M., Gousseinov, E., Kawakami, Y., Laroudie, N., Scanlan, C., Pattnaik, P. (2016) Clarification of vaccines: An overview of filter based technology trends and best practices. *Biotechnol. Adv. 34* (1), 1-13.
5. Kanekiyo, M., Wei, C.-J., Yassine, H. M., McTamney, P. M., Boyington, J. C., Whittle, J. R., Rao, S. S., Kong, W.-P., Wang, L., Nabel, G. J. (2013) Self-assembling influenza nanoparticle vaccines elicit broadly neutralizing H1N1 antibodies. *Nature 499* (7456), 102-106.
6. Feshchenko, E., Rhodes, D. G., Felberbaum, R., McPherson, C., Rininger, J. A., Post, P., Cox, M. M. (2012) Pandemic influenza vaccine: characterization of A/California/07/2009 (H1N1) recombinant hemagglutinin protein and insights into H1N1 antigen stability. *BMC Biotechnol. 12* (1), 1-13.
7. Labrou, N., Clonis, Y. D. (1994) The affinity technology in downstream processing. *J. Biotechnol. 36* (2), 95-119.
8. Roque, A. C. A., Lowe, C. R. (2006) Advances and applications of de novo designed affinity ligands in proteomics. *Biotechnol. Adv. 24* (1), 17-26.
9. Koopmanschap, G., Ruijter, E., Orru, R. V. A. (2014) Isocyanide-based multicomponent reactions towards cyclic constrained peptidomimetics. *Beilstein J. Org. Chem. 10*, 544-598.

10. Haigh, J. M., Hussain, A., Mimmack, M. L., Lowe, C. R. (2009) Affinity ligands for immunoglobulins based on the multicomponent Ugi reaction. *J. Chromatogr. B 877* (14–15), 1440-1452.
11. Chen, C., Khoury, G. E., Lowe, C. R. (2014) Affinity ligands for glycoprotein purification based on the multi-component Ugi reaction. *J. Chromatogr. B 969*, 171-180.
12. El Khoury, G., Wang, Y., Wang, D., Jacob, S. I., Lowe, C. R. (2013) Design, synthesis, and assessment of a de novo affinity adsorbent for the purification of recombinant human erythropoietin. *Biotechnol. Bioeng. 110* (11), 3063-3069.
13. Brownstein, A. (1982) The chemistry of polyethylene glycol, Proceedings of the icom waterlogged wood working group conference p 279-285.
14. Kaur, J., Sharma, R. (2006) Directed Evolution: An Approach to Engineer Enzymes. *Crit. Rev. Biotechnol. 26* (3), 165-199.
15. Uchida, M., Flenniken, M. L., Allen, M., Willits, D. A., Crowley, B. E., Brumfield, S., Willis, A. F., Jackiw, L., Jutila, M., Young, M. J., Douglas, T. (2006) Targeting of Cancer Cells with Ferrimagnetic Ferritin Cage Nanoparticles. *J. Am. Chem. Soc. 128* (51), 16626-16633.
16. Gizeli, E., Lowe, C. R. (2003) *Biomolecular sensors*, pp 78-83, Chapter 4, CRC Press.
17. Bradley, J.-C., Baig Mirza, K., Osborne, T., Wiliams, A., Owens, K. (2008) Optimization of the Ugi Reaction Using Parallel Synthesis and Automated Liquid Handling. *JoVE* (21), 942.
18. Marcaccini, S., Torroba, T. (2007) The use of the Ugi four-component condensation. *Nat. Protoc. 2* (3), 632-639.
19. Li, Z., Kumar, A., Peshkov, A., Van der Eycken, E. V. (2016) A domino Ugi/Michael approach for the synthesis of α,β-unsaturated γ-lactams. *Tetrahedron Lett. 57* (7), 754-756.
20. Hermanson, G. T. (2013) *Bioconjugate techniques* pp 236-237, Chapter 3, Academic press.
21. Lee, S. M. (1989) *Reference book for composites technology Vol. 1*, pp 25-27, Chapter 2, CRC Press.
22. Do, T., Ho, F., Heidecker, B., Witte, K., Chang, L., Lerner, L. (2008) A rapid method for determining dynamic binding capacity of resins for the purification of proteins. *Protein Expression and Purif. 60* (2), 147-150.
23. Li, J., Schantz, A., Schwegler, M., Shankar, G. (2008) Detection of low-affinity anti-drug antibodies and improved drug tolerance in immunogenicity testing by Octet® biolayer interferometry. *J. Pharm. Biomed. Anal. 54* (2), 286-294.
24. Ayyar, B. V., Arora, S., Murphy, C., O'Kennedy, R. (2012) Affinity chromatography as a tool for antibody purification. *Methods 56* (2), 116-129.
25. Dumetz, A. C., Snellinger-O'Brien, A. M., Kaler, E. W., Lenhoff, A. M. (2007) Patterns of protein–protein interactions in salt solutions and implications for protein crystallization. *Protein Sci. 16* (9), 1867-1877.
26. Duong-Ly, K. C., Gabelli, S. B. (2014) Chapter Seven-Salting out of Proteins Using Ammonium Sulfate Precipitation. *Methods Enzymol. 541*, 85-94.
27. Pellaud, J., Schote, U., Arvinte, T., Seelig, J. (1999) Conformation and self-association of human recombinant transforming growth factor-β3 in aqueous solutions. *J. Biol. Chem. 274* (12), 7699-7704.
28. Berne, B. J., Pecora, R. (1976) *Dynamic light scattering: with applications to chemistry, biology, and physics*, pp. 83-86, Chapter 5, Courier Corporation.
29. Hartwig, S., Nguyen, M. M., Hecht, S. (2010) Exponential growth of functional poly (glutamic acid) dendrimers with variable stereochemistry. *Polym. Chem. 1* (1), 69-71.

30. Sundberg, L., Porath, J. (1974) Preparation of adsorbents for biospecific affinity chromatography: I. Attachment of group-containing ligands to insoluble polymers by means of bifunctional oxiranes. *J. Chromatogr. A 90* (1), 87-98.

Table of Contents graphic (TOC)